USING THE DISCRETE ELEMENT METHOD TO ANALYZE AND CALIBRATE A MODEL FOR THE INTERACTION BETWEEN A PLANTING DEVICE AND SOIL PARTICLES
/
栽植器与土壤相互作用离散元模型参数标定及分析

Zeng Fandi, Li Xuying *, Zhang Yongzhi, Zhao Zhiwei, Cheng Cheng [1]
Inner Mongolia Agricultural University, College of Mechanical and Electrical Engineering, Hohhot/China;
Tel: +86-0471-4309215; E-mail: zfd19508@163.com
DOI: https://doi.org/10.35633/inmateh-63-42

Keywords: *Soil, Duckbilled planter, Hertz-Mindlin model, Parameter calibration, Dynamic changes*

ABSTRACT
Dynamic soil behaviour at the contact interface during transplanting makes it difficult to ensure transplanting quality. To solve this problem, the Hertz-Mindlin with bonding contact model was used to calibrate the parameters of soils in Inner Mongolia. Based on the response surface design principle, *four-factor and three-level tests were performed using the repose angle as an evaluation index, and the following influence factors were considered: the soil-soil restoration coefficient, the soil-steel restoration coeficient, the soil-steel static friction coefficient and the soil-steel static friction coefficient. A regression model was analysed, and an optimization procedure yielded the following optimum combination of parameters: a soil-soil restoration coefficient of 0.45, a soil-steel restoration coefficient of 0.35, a soil-steel static friction coefficient of 0.85 and a soil-steel rolling friction coefficient of 0.13. This optimal combination was used to simulate the soil at the contact interface. The particle dynamic behaviour and soil particle mass flow were used to analyse the soil dynamic behaviour, showing that the average mass flow during the gradual opening of the* duckbilled planter *tends to increase over time; when the* duckbilled planter *gradually leaves soil, the contact interface of soil particles in the corner of the* duckbilled planter *unit causes a reduction in the fluctuation range of the soil mass flow, which exhibits a wave-like change. After the duckbilled planter has left soil, the contact interface of the soil changes tends to stabilize. The duckbilled planter-soil discrete element simulation model was verified. The results of this study provide a reference for the optimal design of a duckbilled planter structure.*

摘要
为解决栽植器与接触界面土壤的动态行为造成土壤回流，使栽植质量难以保证等问题，利用 Hertz-Mindlin with Bonding 模型对内蒙地区移栽环境下田间土壤进行参数标定，基于响应面法，分别以土壤-土壤恢复系数、土壤-钢恢复系数、土壤-钢静摩擦系数和土壤-钢滚动摩擦系数为试验因素，进行四因素三水平的正交试验，对回归模型进行了分析，最终得到最佳参数组合为土壤-土壤恢复系数 0.45、土壤-钢恢复系数 0.35、土壤-钢静摩擦系数 0.85 和土壤-钢滚动摩擦系数 0.13；根据最优组合，模拟栽植状态下接触界面的土壤颗粒动态变化行为，进行土壤颗粒质量流量分析，结果表明鸭嘴式栽植器逐渐打开过程中的平均质量流量随着时间的增加呈逐渐增加的趋势，当鸭嘴式栽植器逐渐离开土壤时，鸭嘴式栽植器单位转角内与不同土壤颗粒接触界面变化，土壤质量流量的波动范围较小，呈现波浪式的变化，最终当鸭嘴式栽植器离开土壤，接触界面的土壤质量变化趋于稳定。验证了鸭嘴式鸭嘴式栽植器-土壤离散元仿真模型的正确性，并研究栽植过程中接触土壤的动态变化，为鸭嘴式栽植器结构的优化设计提供参考。

INTRODUCTION

The interaction between a duckbilled planter and the soil is a challenging problem at the contact interface. The discrete element method is used to numerically simulate discrete materials (*Mustafa Ucgul et al., 2014; Lenaerts B. et al., 2014; Li et al., 2016*). The soil particles are modeled as a series of independent motion units; a simulation is performed to obtain the dynamic change law of the soil particles by determining the velocity

[1] *Fandi Zeng, Ph.D. Stud. Eng.; Xuying Li*, Prof. Ph.D. Eng.; Yongzhi Zhang, Lec. Ph.D. Eng.; Zhiwei Zhao, M.S. Eng.; Cheng, M.S. Eng.*

and a force distribution cloud diagram of the interaction between particles and implements; and the motion law of the implements is analysed to provide a reference for the optimal design of agricultural implements (*Fang et al., 2016; Wang et al., 2018*).

Current transplanter research is mostly focused on motion analysis and the working performance of the duckbilled planter. For example, the relationship among the tractor forward speed, the number of cups, the rotational speed of the cups and the planting spacing has been studied by analysing the trajectory of the cups (*Feng et al., 2002*). A 2-row fully automatic vegetable transplanter was developed considering the available power. Test results showed that the field capacity of the transplanter was 0.026 ha h-1, saving 68% of labour and 80% of time compared with traditional manual transplanting, while providing satisfactory transplanting quality (*Kumar et al., 2011*). A semiautomatic tomato transplanter was designed and built with conical distribution cups to increase the speed and precision of cultivation. Test results showed an optimum advance speed and a planting depth of 2 km h^{-1} and 5 cm, respectively. (*Seyed Mohamad Javidan et al., 2019*). The contact interface between the duckbilled planter and soil exhibits complex dynamic behaviour because of the spatial variability of the soil, dynamic factors and soil motion and fragmentation. Many studies on soil discrete element modeling have been carried out in China and abroad: for example, Mustafa used the Hertz-Mindlin and hysteretic spring contact models to analyse the plastic deformation of soil particles with and without cohesive forces (*Mustafa et al., 2015*). Ying Chen used discrete element software to analyse sandy soil mobility (*Ying et al., 2019*). Studies on soil motion in specific situations have shown that the forward speed of tillage implements affects horizontal and lateral soil displacement (*Liu et al., 2010*). Rahman measured the velocity of and disturbance to soil in troughs during various agricultural tillages (*Rahman et al., 2005*). Although the dynamic behaviour of soil during transplanting can deteriorate planting quality, the discrete element model for the interaction between a duckbilled planter and soil has been applied in few studies.

Therefore, the discrete element method was used to calibrate a model of a duckbilled planter and soil particles. The Hertz-Mindlin with bonding contact model was used to carry out soil repose angle tests, and the optimum combination of contact model parameters was determined using the Box-Benhken test. Mass flow was analysed to determine the motion of soil particles from the entry of the duckbilled planter into soil until the planter exits soil; the duckbilled planter-soil discrete element model was verified; and the dynamic changes in the duckbilled planter-soil system during transplanting were elucidated. The research results provide a reference for the optimal design of a duckbilled planter structure.

MATERIALS AND METHODS

- **Basic soil particle parameters**

Soil was selected from the experimental field of the Inner Mongolia Agricultural University in China: the soil had a water content of 14.52% and a density of 1450 kg/m^3, and large particle impurities, such as grass roots, were removed prior to the test. The soil physical parameters were determined in a laboratory at the Institute of Mechanical and Electrical Engineering of the Inner Mongolia Agricultural University. The soil particle size distribution was determined by the sieving method. The soil particle size distribution showed that the soil was a sandy loam.

- **Test method**
- **Soil shear test**

A ZJ-type strain-controlled straight shear instrument is commonly used to determine the shear strength of a soil. This instrument was used to perform experiments on four groups of samples under different vertical pressures (100, 200, 300 and 400 kPa), where the handwheel was gradually rotated to apply a shear force at a speed of 6 r/min until the soil in the shear box was damaged; the soil parameters were then determined using Coulomb's law, which is given by formula (1):

$$\tau = C + \sigma \times tan\varphi \quad (1)$$

Where:

C - Soil cohesion, [kPa];

σ - Normal stress on shear surface, [kPa];

φ - Soil internal friction angle, [°];

The shear strength curve presented in Fig.1 shows that the soil cohesion was 20.46 kPa and the internal soil friction angle was 15.64°.

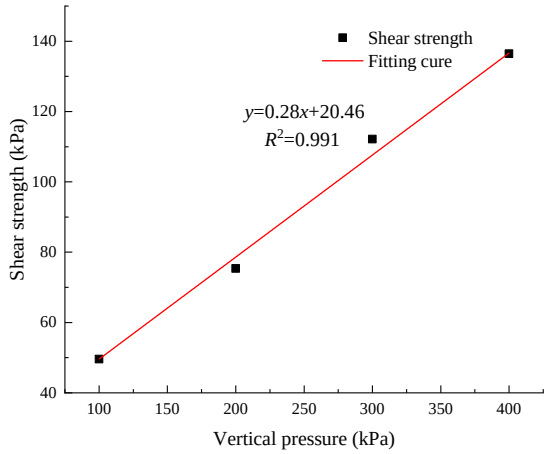

Fig. 1 - Shear strength and vertical load curve

- **Other soil characteristic parameters**

The shear modulus of soil can be approximated using the elastic modulus and Poisson's ratio, where the shear modulus is calculated using formula (2):

$$G=\frac{E}{2(1+\upsilon)} \tag{2}$$

Where:

E - Elastic modulus, [Pa];

υ - Poisson's ratio;

The Poisson's ratio of a soil is the ratio of the lateral expansion strain to the vertical compression strain when the soil is compressed without lateral limits and is typically estimated using formula (3):

$$\upsilon=\frac{K_0}{1+K_0} \tag{3}$$

Where:

K_0 - Side pressure coefficient.

The soil lateral pressure coefficient is the ratio of the lateral pressure to the vertical pressure under lateral pressure conditions and can be approximated using formula (4):

$$K_0=1-\sin\varphi \tag{4}$$

Where:

φ - Soil internal friction angle, [°].

- **Parameter calibration process and analysis**

DEM model of soil particles

An accurate soil particle model ensures the validity of the simulation results. The soil basic structure consists of a block, a nucleus, and column particles (*Zhang et al., 2005*).

The soil particle model is shown in Fig. 2: the model particles in EDEM are spherical, and the spherical filling unit radius is set to 1 mm.

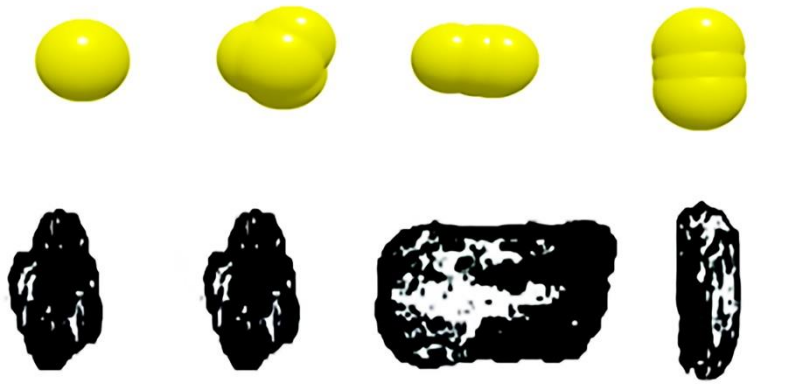

a） lump1 b） lump2 c） nuclei d） columnar

Fig. 2 - Sketch of soil particle model

Contact between soil particles produces a certain degree of bonding that significantly impacts planting resistance and the dynamics of the soil contact interface. The Hertz-Mindlin with bonding contact model was used to decompose the collision forces between soil particles into normal and tangential components, where the particles were bonded together by adding an "adhesive" to prevent relative motion between particles (*Li et al., 2014; Hang et al., 2017*).

When the bonding begins to act on the soil particles, the force Fn and the moments Mn and $M\tau$ of the soil particles increase with the time step, starting from zero, as given in formula (5):

$$\begin{cases} \delta F_{\mathrm{n}} = -V_{\mathrm{n}} S_{\mathrm{n}} A \delta_{\mathrm{t}} \\ \delta F_{\tau} = -V_{\mathrm{r}} S_{\tau} A \delta_{\mathrm{t}} \\ \delta M_{\mathrm{n}} = -\overline{w_n} S_{\mathrm{n}} J \delta_{\mathrm{t}} \\ \delta M_{\tau} = -\overline{w}_{\mathrm{r}} S_{\mathrm{r}} \dfrac{J}{2} \delta_{\mathrm{t}} \\ A = \pi R^2 \\ J = \dfrac{1}{2} \pi R_{\mathrm{b}}^4 \end{cases} \tag{5}$$

Where:

A - Contact area; J- cross-sectional moment of extreme inertia;

S_{n} -Normal stiffness of the bonded particles;

S_{τ} - Tangential stiffness of the bonded particles;

v_{n} - Normal component of the velocity of particle motion;

v_{τ} - Tangential component of particle velocity;

$\overline{w_{\mathrm{n}}}$ - Tangential component of particle angular velocity;

$\overline{w_{\tau}}$- Normal component of particle angular velocity.

The bonding constraint fails when the particle interaction force exceeds a maximum value, as given in formula (6).

$$\begin{cases} \sigma_{\max} < -\dfrac{\mathrm{F_n}}{A} + \dfrac{2M_{\mathrm{t}}}{J} R \\ \tau_{\max} < -\dfrac{F_{\mathrm{t}}}{A} + \dfrac{M_{\mathrm{t}}}{J} \mathrm{R} \end{cases} \tag{6}$$

The Hertz-Mindlin with bonding contact model used in this paper includes five microscopic parameters, namely the normal stiffness S_{n}, the tangential stiffness $S_{\tau,}$ the critical normal stress $\sigma_{\max}$, the bonding tangential critical stress $\tau_{\max}$, and the particle bonding radius R_{b}. The calculations were performed using results from the literature (*Hang et al., 2017*), as shown in Table 1.

Table 1

Contact model parameters

PARAMETER	Value
The normal stiffness	2400000 N/m
The tangential stiffness	1700000 N/m
The critical normal stress	235000 Pa
The bonding tangential critical stress	186000 Pa
Starting time	0.2 s
The particle bonding radius	1.5 mm

- **Simulation parameters**

Existing characteristic material parameters of the soil particles were used in conjunction with measured parameters; the duckbilled planter material is 20 steel with the following parameters: a density of 7850 kg/m^3, a Poisson's ratio of 0.3, and a shear modulus of 7×10^{10}Pa; the remaining parameters were determined using values in the literature (*Dun et al., 2016*), as shown in Table 2. During the simulation, 28% of the Rayleigh time step and the grid size were set to three times the minimum spherical element size.

Table 2

Discrete element simulation parameter table

Simulation parameters	Value
Density of soil particles[kg/m^3]	1452
Poisson's ratio of soil	0.42
Young's modulus of soil [MPa]	1×10^6
Density of steel [kg/m^3]	7850
Poisson's ratio of steel	0.3
Young's modulus of steel [MPa]	7×10^{10}
Soil-soil restitution coefficient	0.15~0.75^a
Soil-soil static friction coefficient	0.4
Soil-soil rolling friction coefficient	0.3
Soil-steel restitution coefficient	0.2~0.5^a
Soil-steel static friction coefficient	0.5~1.2^a
Soil-steel rolling friction coefficient	0.05~0.2^a

Note: a show the term is variable

- **Simulation model for repose angle**

The Hertz-Mindlin with bonding contact model was implemented using the EDEM software and identical inner diameters and heights of the funnel and the cylinder chassis as those used in the repose angle test, as shown in Fig. 3. The particles formed a particle plant at the top of funnel. The particle radius was set to 1 mm, and the simulation generation time was set to 2s. As the lower end of the hopper drop opening remained open, the soil particles continued to fall until all the soil particles stopped moving: a stable particle heap was then formed, and the repose angle was measured.

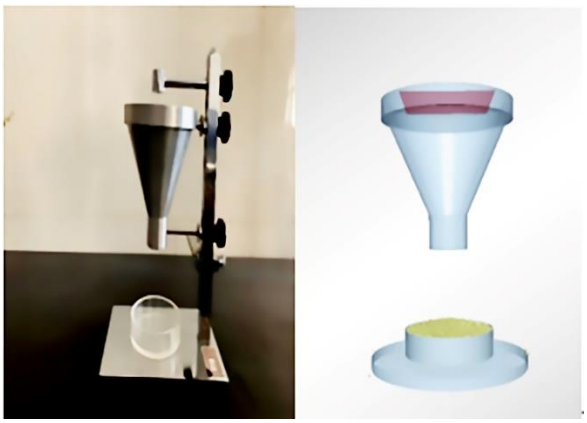

a) Physical test ***b) Simulation test***

Fig. 3 - The repose angle test

- **Response surface design for simulation parameters**

The repose angle parameters were accurately calibrated by determining the contact characteristic parameters (the soil-soil restitution coefficient, the soil-steel restitution coefficient, the soil-steel static friction coefficient and the soil-steel rolling friction coefficient). Based on the response surface design principle, Box-Behnken test was performed and three levels, i.e. low (-1), medium (0) and high (1), was chosen for each parameter. The parameters are shown in Table 3.

Table 3

Factors and levels of the repose angle test

Levels	Soil-soil restitution coefficient A	Soil-steel restitution coefficient B	Soil-steel static friction coefficient C	Soil-steel rolling friction coefficient D
-1	0.15	0.2	0.5	0.05
0	0.45	0.35	0.85	0.13
1	0.75	0.5	1.2	0.2

RESULTS

- **Test results and analysis**

The test scheme consisted of 29 groups of tests, in which each group was repeated three times. The average values were taken as the test results. The results are shown in Table 4.

Table 4

Test scheme and results of repose angle

No.	Soil-soil restitution coefficient A	Soil-steel restitution coefficient B	Soil-steel static friction coefficient C	Soil-steel rolling friction coefficient D	Angle of repose
	/	/	/	/	[°]
1	0.15	0.35	0.85	0.20	26.13
2	0.15	0.20	0.85	0.13	28.31
3	0.45	0.35	0.50	0.05	30.39
4	0.45	0.35	1.20	0.05	26.59
5	0.75	0.35	0.85	0.20	30.26
6	0.45	0.35	0.85	0.13	34.03
7	0.45	0.35	0.85	0.13	33.93
8	0.15	0.50	0.85	0.13	29.69
9	0.45	0.35	1.2	0.20	31.23
10	0.45	0.35	0.85	0.13	34.66
11	0.45	0.35	0.85	0.13	33.76
12	0.45	0.35	0.85	0.13	34.49
13	0.75	0.35	0.50	0.13	26.56
14	0.45	0.20	0.85	0.20	30.43
15	0.15	0.35	1.20	0.13	28.96
16	0.75	0.35	0.85	0.05	30.29
17	0.15	0.35	0.85	0.05	28.49
18	0.75	0.20	0.85	0.13	25.96
19	0.75	0.35	1.20	0.13	30.59
20	0.45	0.50	1.20	0.13	29.36
21	0.45	0.50	0.85	0.05	30.13
22	0.15	0.35	0.5	0.13	28.80
23	0.45	0.35	0.5	0.20	30.96
24	0.45	0.20	0.5	0.13	28.59
25	0.45	0.20	1.2	0.13	32.26
26	0.45	0.50	0.5	0.13	30.23
27	0.45	0.20	0.85	0.05	28.89
28	0.75	0.50	0.85	0.13	29.83
29	0.45	0.50	0.85	0.20	31.46

- **Analysis of variance and the regression model**

The test results were analysed using design-expert 8.0.6, and the ANOVA results are shown in Table 5. The regression model for the repose angle is shown in formula (7). The letters *A*, *B*, *C* and *D* correspond to parameters with a highly significant effect on the repose angle, where the order of influence on the repose angle was soil-steel restitution coefficient *B*<soil-steel static friction coefficient *C*<soil-steel rolling friction coefficient *D*<soil-soil restitution coefficient *A*. The interaction terms *AB*, *AD*, *BC* and *CD* were found to have an important effect on the repose angle. The analysis of variance results show that the model was extremely significant (*P*<0.01).

$$\theta=34.17+1.48A+0.57B-0.88C+1.30D+0.62AB+0.47AC+0.58AD-0.64BC-0.052BD+1.02CD$$
$$-3.50A^2-2.06B^2-2.50C^2-1.88D^2-0.75A^2B+2.43A^2C-1.90A^2D-2.03AB^2$$
$$-1.14AC^2+1.08B^2C-0.59B^2D-0.38BC^2-0.16A^2B^2+0.053A^2C^2$$

Table 5

ANOVA of soil repose angle model of Box-Benhken test

Source	DF	MS	F Value	P Value
Model	24	6.98	47.52	< 0.0001**
A	1	8.79	59.83	0.0015
B	1	1.29	8.77	0.0415
C	1	3.12	21.20	0.0100
D	1	6.79	46.19	0.0024
AB	1	1.55	10.55	0.0314
AC	1	0.87	5.95	0.0713
AD	1	1.36	9.24	0.0384
BC	1	1.61	10.98	0.0296
BD	1	0.011	0.075	0.7977
CD	1	4.14	28.19	0.0061
A^2	1	25.12	170.97	0.0002
B^2	1	17.95	122.14	0.0004
C^2	1	26.31	179.03	0.0002
D^2	1	14.91	101.50	0.0005
A^2B	1	1.11	7.55	0.0514
A^2C	1	11.81	80.38	0.0009
A^2D	1	7.22	49.14	0.0022
AB^2	1	8.28	56.37	0.0017
AC^2	1	2.58	17.54	0.0138
B^2C	1	2.34	15.95	0.0162
B^2D	1	0.68	4.66	0.0971
BC^2	1	0.29	1.99	0.2310
A^2B^2	1	0.026	0.18	0.6934
A^2C^2	1	2.756E-003	0.019	0.8977
Pure Error	4	0.15		
Cor Total	28			
R^2=0.996; R^2_{adj}=0.975; CV=1.28%; Adeq-Precision=23.08				

*Note: P < 0.01 (extremely significant, **),P < 0.05 (significant, *).*

- **Analysis of influences of interaction factors on productivity**

The optimized regression equation was solved using the actual repose angle of the soil particles as a target. The ANOVA results of the regression model indicated that parameter interaction terms, i.e. AB, AD, BC and CD, had a significant effect on the repose angle of the soil particles (*P*<0.05). The response surfaces of the four considered parameters under the interactions of AB, AD, BC and CD were plotted using design expert software, as shown in Fig. 4, to analyse the effect of the interaction terms on the repose angle.

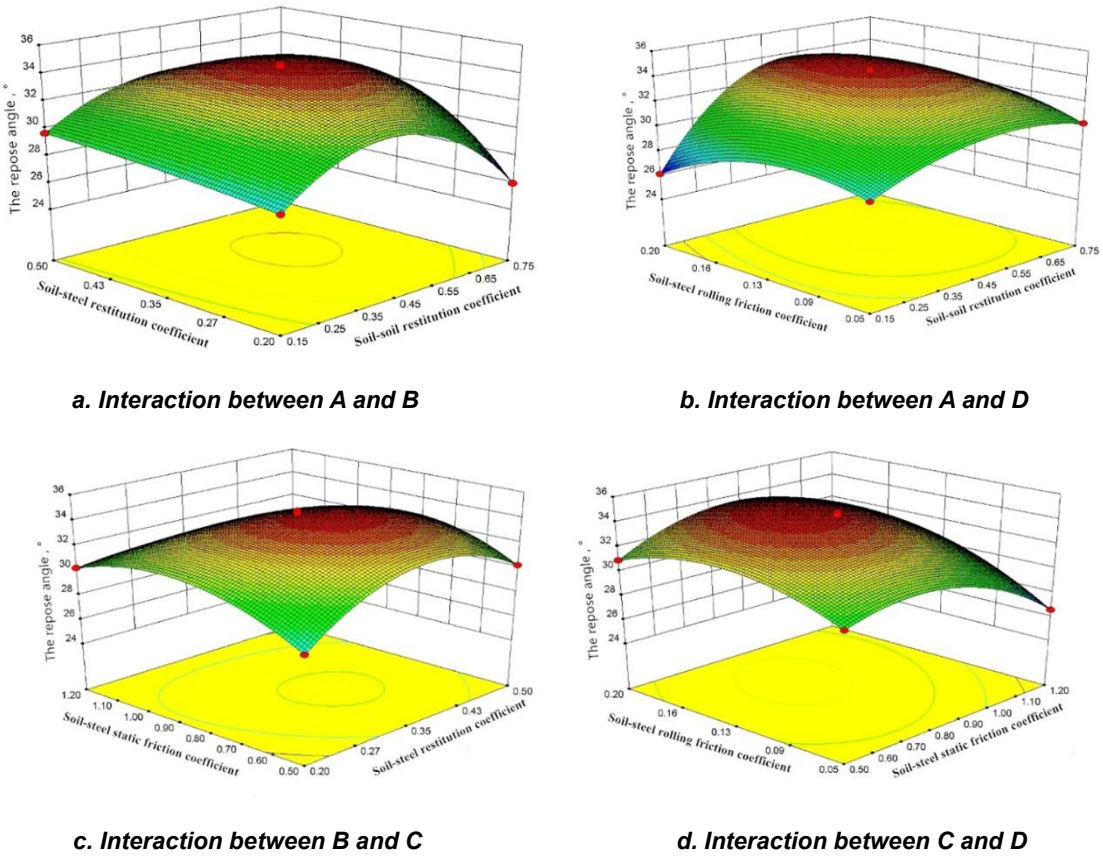

a. Interaction between A and B *b. Interaction between A and D*

c. Interaction between B and C *d. Interaction between C and D*

Fig. 4 – Interaction effect diagram of response surface results

Fig. 4a-4d show the response surfaces of the soil-soil restitution coefficient, the soil-steel restitution coefficient, the soil-steel static friction coefficient and the soil-steel rolling friction coefficient with respect to the repose angle: when the soil-steel rolling friction coefficient and the soil-steel static friction coefficient were at the zero position, the soil-steel recovery coefficient and the soil-soil recovery coefficient increased, whereas the repose angle first increased and then decreased (Fig. 4a); when the soil-steel restitution coefficient and the soil-steel static friction coefficient were at the zero position, the soil-soil restitution coefficient and the soil-steel rolling friction coefficient increased, whereas the repose angle first increased and then decreased (Fig. 4b); for a soil-steel restitution coefficient of 0.35, the repose angle slowly increased (Fig. 4c). For a soil-steel rolling friction coefficient of 0.13, the repose angle decreased with the soil-steel static coefficient (Fig. 4d).

- **Parameter optimization and verification**

To obtain the optimal parameters of the repose angle, the regression equation was solved using design-expert 8.0.6 software. The objective function and constraints are given in formula (7).

$$\begin{cases} max\theta \\ 0.15 \le A \le 0.75 \\ 0.2 \le B \le 0.5 \\ 0.5 \le C \le 1.2 \\ 0.05 \le D \le 0.2 \end{cases} \quad (7)$$

The optimization procedure yielded the following optimum combination of parameters for the repose angle: a soil-soil restitution coefficient of 0.45, a soil-steel restitution coefficient of 0.35, a soil-steel static friction coefficient of 0.85 and a soil-steel rolling friction coefficient of 0.13. The predicted repose angle was 34.71°. The reliability of the prediction was verified by carrying out a physical test: the measured repose angle of 36.23° showed that the prediction model was reliable.

- **Dynamics of soil particles at contact interface during planting**
- **Simulation model for transplanting**

The dynamic changes in soil at the contact interface were determined by using EDEM in the simulation. The transplanting depth for tomatoes and other agricultural crops was generally 60 ~ 100 mm, and a prism-type duckbilled planter was selected, as shown in Fig. 5. Considering that the soil surface in an actual field is uneven, the soil particle was set to 3 mm, and the final plane of naturally fallen soil particles was regarded as flat soil in the simulation, thereby increasing the calculation speed and saving computing time.

Taking λ = 1.068 as an example, the transplanting operation was set to begin at 5 s, and the angular velocity of the duckbilled planter was set at 1.57 rad/s; the dynamic simulation of soil particles at the contact interface under the operation state of the transplanter was then carried out. The simulation model is shown in Fig. 6, where the simulation was completed in 8 s: information about the soil mass flow was collected using the mass flow sensor during post-processing.

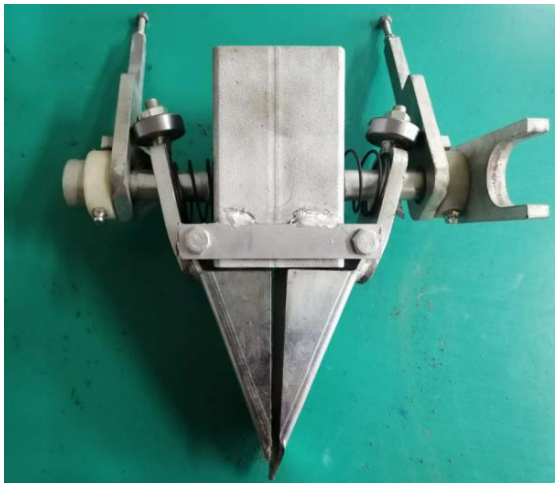

Fig. 5 - A prism-type duckbilled planter

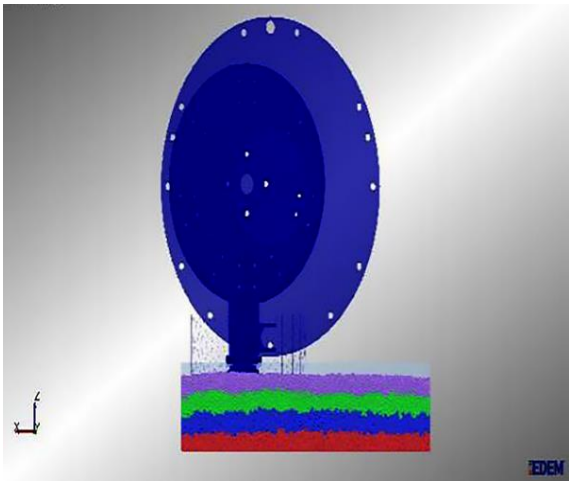

Fig. 6 - Mass flow statistics diagram

- **Velocity analysis of soil movement at contact interface**

A simulation time of 8 s was used. After the simulation was completed, a post-processing colouring function was used to mark the speed of the soil particles to determine the dynamic changes of the particles, where the colours were set to black, red and gray.

Soil particle velocity cloud maps and vector cloud maps at two points were used in the simulation: the lowest position that the duckbilled planter penetrates to and the position at which the duckbilled planter is maximally open, as shown in Figs. 7 and 8.

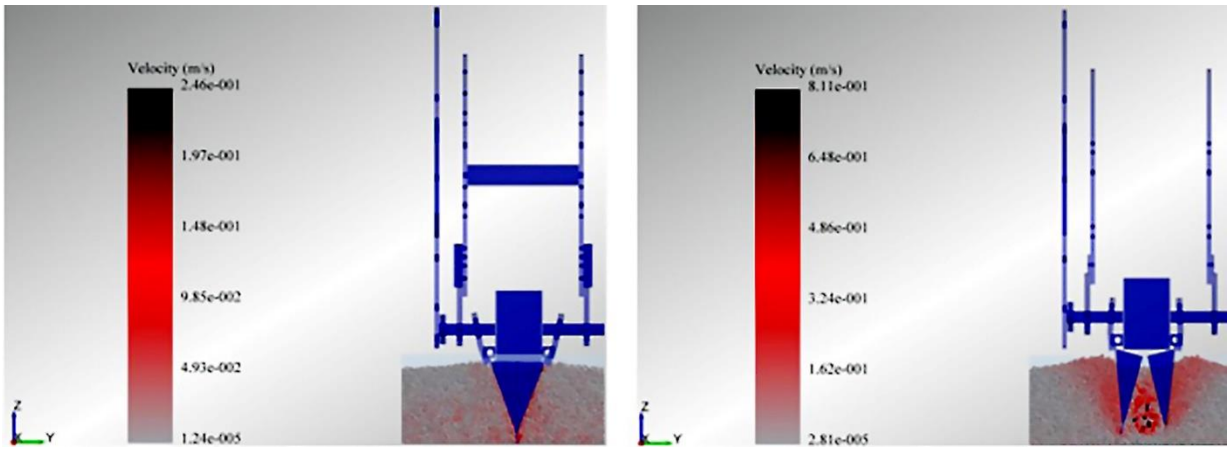

a. The duckbilled planter reaches the lowest point ***b. The duckbilled planter is maximally open***

Fig. 7 - Soil particle velocity cloud maps

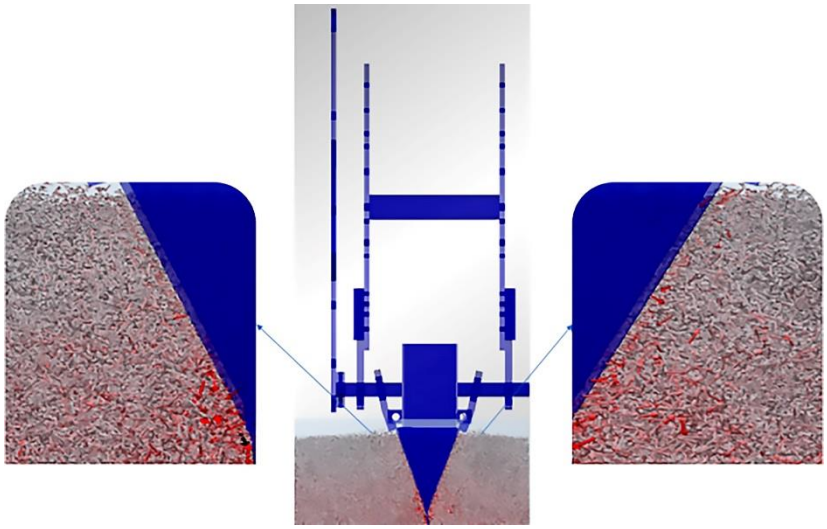

a. The duckbilled planter reaches their lowest point

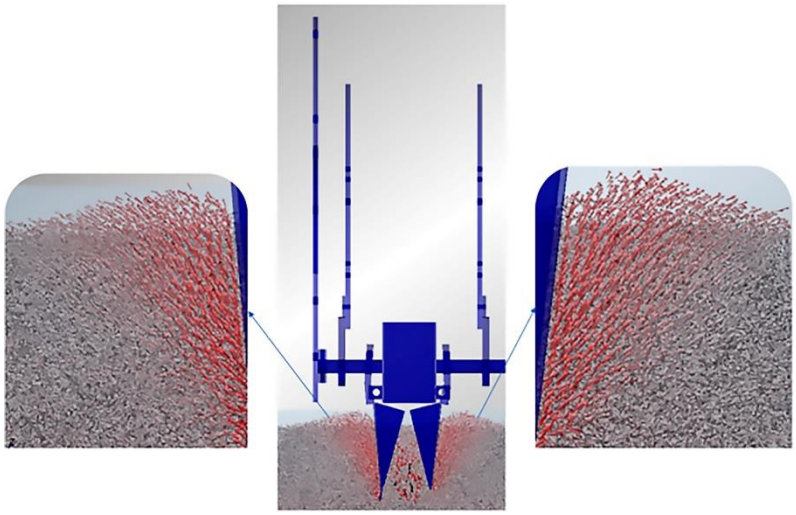

b. The duckbilled planter is maximally open

Fig. 8 - Soil particle velocity vector cloud maps

The velocity of soil particles close to the squeezing action of the duckbilled planter after the planter has reached its lowest point of penetration is smaller than the velocity of soil particles away from the duckbilled planter. As shown in Fig. 7a and 7b, the maximum velocity of soil particles at the contact interface is 0.10279 and 0.26138 m/s at the lowest point of the duckbilled planter and at the maximum opening of the duckbilled planter, respectively. Fig. 8a and 8b clearly shows that the velocity vector of the soil particle population at the contact interface points away from the duckbilled planter and outward towards the outer wall of the beak. As the duckbilled planter gradually opens, soil particles gather around the planter beak. When the duckbilled planter is at its maximum opening during transplanting, the soil at the contact interface is clearly moving opposite to the direction of the transplanting speed, indicating reflux and flow into the bottom of the hole.

- **Soil particle mass flow analysis at contact interface**

The opening and closing of the duckbilled planter during transplanting significantly affects soil dynamics. Thus, the motion of the entire soil particle system, from the duckbilled planter to the soil discharge process, must be simulated and analysed, where the mass flow is used to describe the dynamics of the soil particles. The reference surface level in the simulation is taken to be the final stable surface of the falling particles after the filling phase of the soil particles, where the mass flow is 0 kg/s. The mass flow sensor is used during post-processing of the discrete element software to collect data on the average mass flow rate of the soil particles at the contact interface, which is then used to derive the variation curve for the average mass flow shown in Fig. 9.

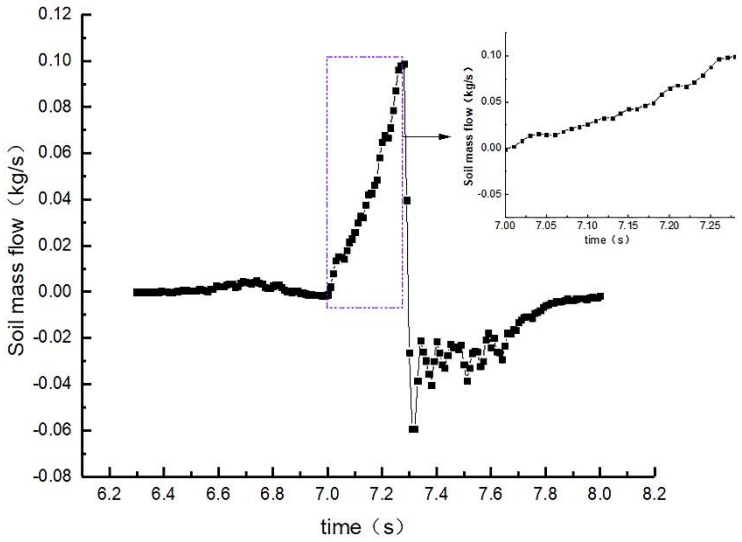

Fig. 9 - Soil mass flow versus time curve

The mass flow of soil particles at the contact interface changes slightly between when the duckbilled planter first touches the soil and the duckbilled planter reaches its lowest point of penetration; when the duckbilled planter completes drilling and the seedlings are planted, the soil particles at the contact interface are affected by the rotational motion of the duckbilled planter with a rotating spindle and the forward speed of the tractor, as well as by the opening motion of the duckbilled planter at the lowest point of penetration. The enlarged diagram shows different effective depths of the duckbilled planter in contact with the soil for different positions of the planter during the opening of the planter; the change in the contact space between the duckbilled planter and the contact interface of soil particles results in different soil particle masses per unit corner. As the duckbilled planter opens, the mass flow of soil particles at the contact interface increases over time. When the duckbilled planter opens to its maximum extent, as shown in Fig. 9, the soil particles at the contact interface are in contact with the bulk soil. At this time, the duckbilled planter gradually leaves the soil in this maximally open state because the soil particles at the contact interface are subjected to the effect of the rotational motion of the duckbilled planter, which acts in conjunction with the rotating spindle and the tractor traction to produce a flattening motion; however, the soil particles at the interface on both sides of the planter are no longer subjected to the planter opening motion, and the opening of the duckbilled planter exerts a force on the soil on both sides of the planter to change the dynamics of the surface soil particles. This force causes the curve to change abruptly, such that the soil mass flow at the contact interface exhibits a wave-like change under the movement and inertia of the soil. The duckbilled planter eventually leaves the soil, and the soil mass flow at the contact interface stabilizes at -0.00187 kg/s.

CONCLUSIONS

1. A straight shear test was used to determine the soil characteristics of a field in Inner Mongolia: the soil cohesion was 20.46kPa and the friction angle was 15.64°, which provided an empirical basis for a discrete element model of the interaction between soil and a duckbilled planter.

2. An optimization procedure was performed to determine the following optimum combination of parameters: a soil-soil recovery coefficient of 0.45, a soil-steel recovery coefficient of 0.35, a soil-steel static friction coefficient of 0.85 and a soil-steel rolling friction coefficient of 0.13; the simulation model was found to accurately reflect the physical characteristics of the soil in the Inner Mongolia field environment.

3. EDEM software was used to analyse the soil dynamics at the contact interface. The mass flow of soil changed slightly during transplanting. At the seedling stage, the soil mass flow trended upwards with time. When the duckbilled planter opened to its maximum extent and then gradually left the soil, the soil mass flow exhibited a wave-like change. After the duckbilled planter left the soil, the soil mass flow tended to stabilize.

ACKNOWLEDGEMENTS

This project was funded by the National Natural Science Foundation of China (NSFC) (51465048) and the Natural Science Foundation of the Inner Mongolia Autonomous Region of China (2019MS05031 and 2020MS05055).

REFERENCES

[1] Dun, Guoqiang, Chen, Haitao, Feng, Ying et al. (2016). Parameter optimization and experiment of key components of fertilizer blending device based on EDEM software. *Transactions of the Chinese Society of Agricultural Engineering*, 32(7), 36-42. https://doi.org/ 10.11975/j.issn.1002-6819.2016.07.005

[2] Fang, Huimin, Zhang, Qingyi, Farman, Ali Chandio et.al. (2016). Effect of straw length and rotavator kinematic parameter on soil and straw movement by a rotary blade. *Engineering in Agriculture, Environment and Food*, 9(3), 235-241. https://doi.org/10.1016/j.eaef.2016.01.001

[3] Feng, Jun, Qin, Gui, Song, Weitang et al. (2002). Analysis and design criteria of hanging cup movement of transplanting machine. *Transactions of the Chinese Society of Agricultural Machinery*, 33(5), 48-50. https://doi.org/10.3969/j.issn.1000-1298.2002.05.015

[4] Hang, Chengguang, Huang, Yuxiang, Zhu, Ruixiang, (2017). Analysis of the movement behaviour of soil between subsoilers based on the discrete element method. *Journal of Terramechanics*, 74(12), 35-43. https://doi.org/10.1016/j.jterra.2017.10.002

[5] Hang, Chengguang, Gao, Xijie, Yuan, Mengchang et al. (2017). Discrete element simulations and experiments of soil disturbance as affected by the tine spacing of subsoiler. *Biosystems Engineering*, 168, 73-82. https://doi.org/10.1016/j.biosystemseng.2017.03.008

[6] Kumar, G. V. P., Raheman, H., (2011). Development of a walk-behind type hand tractor powered vegetable transplanter for paper pot seedlings, *Biosystems Engineering*, 110(2), 189-197. https://doi.org/10.1016/j.biosystemseng.2011.08.001.

[7] Lenaerts, B., Aertsen, T., Tjskens, E. et al. (2014). Simulation of grain-straw separation by discrete element Modelling with bendable straw particles. *Computers & Electronics in Agriculture*, 101, pp.24-33. https://doi.org/10.1016/j.compag.2013.12.002

[8] Li, Bo, Liu, Fanyi, Mu, Junying et al. (2014). Distinct element method analysis and field experiment of soil resistance applied on the subsoiler. *International Journal of Agricultural and Biological Engineering*, 7(1), 54-59. https://doi.org/10.3965/j.ijabe.20140701.006

[9] Li, Bo, Chen, Ying, Chen, Jun (2016). Modelling of soil–claw interaction using the discrete element method (DEM). *Soil & Tillage Research*, *158*(1), 177-185. https://doi.org/10.1016/j.still.2015.12.010

[10] Liu, J., Chen, Y., Kushwaha, R. L., (2010). Effect of tillage speed and straw length on soil and straw movement by a sweep. *Soil & Tillage Research*, 109(1), 9-16. https://doi.org/10.1016/j.still.2010.03.014

[11] Qi Long, Chen Ying, Sadek, Mohammad, (2019). Simulations of soil flow properties using the discrete element method (DEM). *Computers and Electronics in Agriculture*, 157, 254-260. https://doi.org/10.1016/j.compag.2018.12.052

[12] Ucgul, M., Fielke, J. M., Saunders, C. (2014). 3D DEM tillage simulation: validation of a hysteretic spring (plastic) contact model for a sweep tool operating in a cohesionless soil. *Soil & Tillage Research*, 144, 220-227. https://doi.org/10.1016/j.still.2013.10.003

[13] Ucgul, M., Fielke, J. M., Saunders, C., (2015). Defining the effect of sweep tillage tool cutting edge geometry on tillage forces using 3D discrete element modelling. *Information Processing in Agriculture*, *2*(2), 130-141. https://doi.org/10.1016/j.inpa.2015.07.001

[14] Rahman, S., Chen, Y., Lobb, D. A., (2005). Soil movement resulting from sweep type liquid manure injection tools. *Biosystems Engineering*, 91(3), 379-392. https://doi.org/10.1016/j.biosystemseng.2005.04.002

[15] Seyed Mohamad Javidan, Davood Mohammadzamani, (2019). Design, construction and evaluation of semi-automatic vegetable transplanter with conical distributor cup. *SN Applied Sciences*. 1(9). https://doi.org 10.1007/s42452-019-1034-y

[16] Wang, Xuezhen, Yue, Bin, Gao, Xijie et al. (2018). Simulation and experiment of soil disturbance behaviour of deep loose shovel with different wing shovel installation heights. *Journal of Agricultural Machinery*, vol.49 (10), pp.124-136. https://doi.org/10.6041/j.issn.1000-1298.2018.10.014

[17] Zhang, Rui, Li, Jiangqiao, (2006). Simulation on mechanical behaviour of cohesive soil by distinct element method. *Journal of Terramechanics*, *43*(3), 303-316. https://doi.org/10.1016/j.jterra.2005.05.006